The University of Texas Libraries - Interlibrary Services - **IXA**

Ph: 512-495-4131 **Fax**: 512-495-4283 **Ariel:**128.83.206.11

Borrower: MUB

ILL: 10389572 **ILLiad TN: 254951**

Lending String: *IXA,IXA,LHL,MYG,WAU

Patron: DEPT; STATUS; Gobbert, Matthias

Journal Title: Plasma processing XIV ; proceedings of the International Symposium /

Volume: 2002-17 **Issue:**
Month/Year: 2002
Pages: 25-34 copy of chapter

Article Title: Vinay Prasad, Matthias K. Gobbert, and Timothy S. Cale; Optimizing Pulse Protocols in Plasma-Enhanced Atomic Layer Deposition

Article Author: International Symposium on Plasma Processing (14th ; 2002 ; Philadelphia, Pa.)
Imprint: Pennington, NJ ; Electrochemical Society

Call #: TA 2020 S95 2002
Location: CHEM

ARIEL
Charge
Maxcost: $20IFM

Shipping Address:
University of Maryland, Baltimore County
Albin O. Kuhn Library and Gallery
1000 Hilltop Circle
Baltimore, MD 21250

Fax:
Ariel: 130.85.150.114

CONCLUSIONS

By using an ultraclean ECR plasma apparatus, Atomic-order Nitridation of Si(100) is controlled by nitrogen radical exposure. High quality Si epitaxial growth is also realized by Ar^+ ion-assisted SiH_4 reaction without substrate heating. In the case after nitridation, epitaxial Si film can be grown even on the about $1.6 \times 10^{15} cm^{-2}$ nitrided Si(100). Depth profile of the N concentration in the N-doped Si epitaxial film shows that N atoms are confined within 1.6nm-thick region with the N concentration is about $6 \times 10^{21} cm^{-3}$, and it is shown that the ECR plasma process is effective to achieve the extremely high concentration N doping in Si crystal.

ACKNOWLEDGMENTS

This study was partially supported by the Public Participation Program for the Promotion of Info. Communications Technology R&D from the Telecommunications Advancement Organization of Japan, JSPS Research for the Future Program (#JSPS-RFTF97P00202), and a Grant-in-Aid for Scientific Research from the Ministry of Education, Culture, Sports, Science and Technology of Japan.

REFERENCES

[1] T.Seino, T.Matsuura, and J.Murota, Appl. Phys. Lett. 76, 342 (2000).
[2] K.Fukuda, J.Murota, S.Ono, T.Matsuura, H.Uetake, and T.Ohmi, Appl. Phys. Lett. 59, 2853 (1991).
[3] D.Muto, T.Seino, T.Matsuura, and J.Murota, American Vacuum Society 48th Int. Symp., San Francisco, CA, USA, Oct.28-Nov.2, 2001, Abs.No. EL-WeA3.
[4] T.Matsuura, Y.Honda, and J.Murota, Appl. Phys. Lett. 74, 3573 (1999).
[5] T.Seino, D.Muto, T.Matsuura, and J.Murota, American Vacuum Society 47th Int. Symp., Bostion, Massachusetts, USA, Oct. 2-6, 2000, Abs.No.PS-WeP17.
[6] T.Seino, T.Matuura, and J.Murota, Surf. Interface Anal. 34, (2002) (in press).

OPTIMIZING PULSE PROTOCOLS IN PLASMA-ENHANCED ATOMIC LAYER DEPOSITION

[1]Vinay Prasad, [2]Matthias K. Gobbert, and [1]Timothy S. Cale

[1]Focus Center - New York, Rensselaer: Interconnections for Gigascale Integration, Rensselaer Polytechnic Institute, CII 6015, 110 8th Street, Troy, NY 12180-3590

[2]Department of Mathematics and Statistics, University of Maryland, Baltimore County, 1000 Hilltop Circle, Baltimore, MD 21250

We use a transient, Boltzmann equation based transport and reaction model to study atomic layer deposition (ALD) at the feature scale, and focus on improving pulse protocols. We use this model to simulate plasma-enhanced ALD and to explain growth rate dependence on pulse times for two different processes for TBTDET sourced TaN recently reported in Park *et al.*, J. Electrochem. Soc., 149(1), C28 (2002); ALD using ammonia as the co-reactant and plasma-enhanced ALD using a hydrogen plasma. We use the calibrated chemistry models to predict surface coverage and monolayers deposited over several ALD cycles. We conclude that the monolayers per cycle can be increased relative to the experimental data by shortening the post-adsorption purge time; this decreases reactant desorption. The overall growth rate can by increased by decreasing co-reactant and post-reaction purge pulse times; they are longer than necessary.

INTRODUCTION

Atomic layer deposition (ALD) has attracted attention because of the possibility of self-limiting, monolayer-by-monolayer depositions [1-4]. Due to the periodic pulsing of reactants and purge gases, a comprehensive model for ALD should start with the transient nature, and include models for gas phase transport and surface chemistry. Much of the relevant literature on feature scale modeling of ALD consists of descriptions of surface mechanisms without a model for gas phase transport [5, 6]. The dominant approach to feature scale transport and reaction analyses was developed to model topography evolution during conventional steady-state deposition and etch processes. These models are pseudo-steady, *i.e.*, the local surface reaction rates are computed assuming fluxes are constant in time [7]. EVOLVE [7, 8] offers a comprehensive framework for feature scale topography simulation during pseudo-steady deposition and etch processes, but is apparently not appropriate for ALD. We have developed a transient, Boltzmann equation based transport and reaction model for ALD [9-12]. The transport model has no adjustable parameters, and heterogeneous reaction mechanisms are used to express

adsorption, desorption, and surface reaction. Results for the adsorption and post-adsorption purge steps, and for the reaction and post-reaction purge steps are presented in [10, 11]. We focus on the feature scale and idealize changes at the reactor scale, *i.e.*, changes in flow and concentrations are assumed to occur such that changes directly over the feature can be considered to occur as step functions. Thus, all fluxes from the reactor volume to the feature mouth are constant in time, except for step changes at the start of a pulse.

In this work, we extend the use of the ALD simulator to model deposition in plasma-enhanced ALD; i.e., to include ions in the transport model. Plasma-enhanced ALD (PEALD) has recently been investigated [13-15] as a possible method to increase surface reaction rates and improve deposited film properties. In Refs. 14 and 15, tantalum nitride (TaN) was deposited using tertbutylimidotris(diethylamido)tantalum (TBTDET) as a precursor, and hydrogen radicals were used as reducing agents. Films formed using PEALD were found to exhibit better properties (lower electrical resistivity, no aging effects under exposure to air) than those formed using conventional ALD (with NH_3 as a reducing agent) [15]. We fit kinetic parameters in our model to interpret experimental data on the dependence of deposition rates on reactant pulse times for TaN ALD as described in Ref. 15.

MODEL

Feature Scale Transport Model

For this paper, we consider the two-dimensional cross-section of a feature with aspect ratio $A = 4$, as shown in Fig. 1. The width of the feature mouth is taken as $L = 0.25$ μm. The domain consists of the interior of the feature and a small area of gas inside the Knudsen layer above the wafer surface.

The transport of the inert carrier gas I and the reactive species through the domain is described by a set of Boltzmann transport equations (BTEs). Assuming that the reactive species are at least an order of magnitude less concentrated than the carrier gas, it is possible to decouple the BTE for the inert I, and we only have to solve a system of BTEs for the reactive species [10, 11].

We assume that the inflow conditions at the interface to the bulk of the reactor chamber are specified and homogeneous in space and time. For neutral species, we use a Maxwellian distribution. At the sides of the domain above the wafer surface, we use specular reflection to simulate periodic features. At the wafer surface, we model the emission of gaseous molecules into the computational domain as diffusive emission by prescribing a Maxwellian velocity distribution for neutral species. In the absence of reactions, the inflowing density distribution is modeled as being proportional to the flux to the surface for each species η_i; if reactions are present, the rates R_i of the surface reactions increase or decrease the inflowing density distribution.

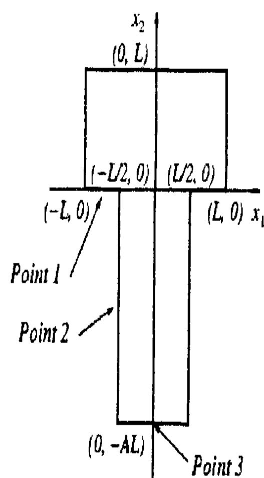

Figure 1. Schematic of a two-dimensional domain defining length L and aspect ratio A.

The BTEs are nondimensionalized using reference quantities for concentration and speed of the reactant species [10, 11]. The reference concentration and speed are chosen to be the corresponding quantities for A, the first reactive species, at the conditions listed in the Results section. Since we seek to compare model predictions of deposition rates with experimental data from Ref. [15], the first reactive species is TBTDET, the organometallic precursor used for TaN ALD.

Surface Reaction Model

The surface chemistry model accounts for reaction of TBTDET with radicals in the hydrogen plasma used in TaN PEALD. We designate hydrogen radicals to be the second reactive species (B). Ions are the third gaseous species; however, we do not consider them in the surface reaction model. We justify this in the next section. Our surface reaction model consists of reversible adsorption of A on a single site, and irreversible reaction of B with the adsorbed A

$$A + v \Leftrightarrow A_v$$
$$A_v + B \rightarrow v + (*) \tag{1}$$

where A_v is adsorbed A, v stands for a surface site available for adsorption, and (*) is the non-adsorbing gaseous product. Surface sites for adsorption are produced by the reaction of B with adsorbed A.

If the fraction of surface sites occupied by molecules of species A is denoted by ϑ_A, the reaction rates, made dimensionless by dividing them by the flux of species A to the wafer well away from any feature [10, 11], can be written as

$$R_1 = \gamma_1^f (1-\vartheta_A)\eta_1 - \gamma_1^b \vartheta_A$$
$$R_2 = \gamma_2^f \vartheta_A \eta_2 \tag{2}$$

where η_i denotes the (dimensionless) flux of species i to the surface, and γ_1^f, γ_1^b, and γ_2^f are (dimensionless) rate parameters associated with adsorption, desorption, and reaction of A with B, respectively. The dimensionless fluxes and reaction rates can be re-dimensionalized by multiplying them by the flux of species A. The dimensionless rate parameters can be re-dimensionalized using the flux of species A and the total number of sites available for adsorption per unit area.

The evolution of ϑ_A at every point of the wafer surface is given by

$$\frac{d\vartheta_A(t)}{dt} = \alpha_p (R_1(t) - R_2(t)), \;\; \vartheta_A(0) = \vartheta_A^{ini} \tag{3}$$

where the initial coverage ϑ_A^{ini} is known and α_p is a constant prefactor arising from the non-dimensionalization procedure. In general, this differential equation cannot be solved

in closed form, because its coefficients depend on the fluxes η. However, if we can justify the assumption that the fluxes are constant in time, an analytic solution for the fractional coverage ϑ_A can be obtained (see [10, 11]).

RESULTS

The experimental data we calibrate our model against were obtained from Park *et al.* [15], who conducted a comparison of ALD using NH_3 as the reducing agent, and (hydrogen) plasma enhanced ALD. To ignite and maintain the hydrogen plasma synchronized with the deposition cycle, a rectangular shaped pulse of power was applied between the upper and lower electrode. The lower electrode, on which a wafer resided, was grounded. The upper electrode was of a showerhead type to distribute reactant gases uniformly, and was operated at 50-150 W power, capacitively coupled with an rf (13.56 MHz) power generator [15].

In the experiments reported by Park *et al.* [15], TBTDET was used as the precursor. It was contained in a bubbler that was heated to 70 °C; argon was used as the carrier gas, at a flow rate of 35 cm^3/min. One deposition cycle consisted of an exposure to TBTDET, a purge period with an argon flow rate of 35 cm^3/min, an exposure to hydrogen plasma, followed by another purge period with an argon flow rate of 35 cm^3/min. The hydrogen flow rate was fixed at 75 cm^3/min during the hydrogen plasma pulse. The deposition temperature was 260 °C, and the deposition pressure was 1 Torr. For the case of ALD, ammonia was used as the reducing agent in place of hydrogen radicals. The flow rate of NH_3 was fixed at 47 cm^3/min. The TBTDET pulse time was varied between 1 s and 6 s. All the purge times were 15 s long, and the NH_3 and hydrogen plasma pulses were 10 s long in ALD and PEALD, respectively. The reference concentration and speed of TBTDET at these conditions are 1.5×10^{-9} mol/cm^2 and 1.05×10^4 cm/s respectively.

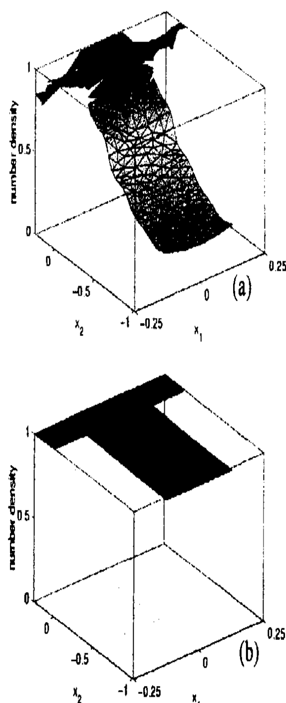

Figure 2. TBTDET adsorption step: dimensionless number density of species A for a feature with aspect ratio $A = 4$ at (a) 5.0 ns, (b) 40.0 ns. The scales on the x_1 and x_2 axes are different.

Figures 2*a* and 2*b* show representative distributions of the dimensionless number density of TBTDET throughout the gas domain during the adsorption step at $t = 5$ ns and 40 ns. After 5 ns, the gas has not filled the interior of the feature yet; after 40 ns the feature has filled completely with gas. This demonstrates that the transport is much faster than the duration of the adsorption step. Similarly, the gas is transported out of the feature domain over a time scale much shorter than the duration of the pulse during the post-adsorption purge. Figure 3 shows the flux to the surface of species A vs. time at the three observation points (see Fig. 1); Fig. 3*a* for the adsorption step and Fig. 3*b* for the post-adsorption purge step. Observe that in both processing steps, the flux tends to equilibrium more slowly than the gas fill of the domain, but significantly faster than the total step times for adsorption and post-adsorption purge. Additionally, observe that the fluxes tend to a spatially uniform constant value. For similar and more detailed results on the adsorption and post-adsorption purge steps of ALD, see Ref. 10.

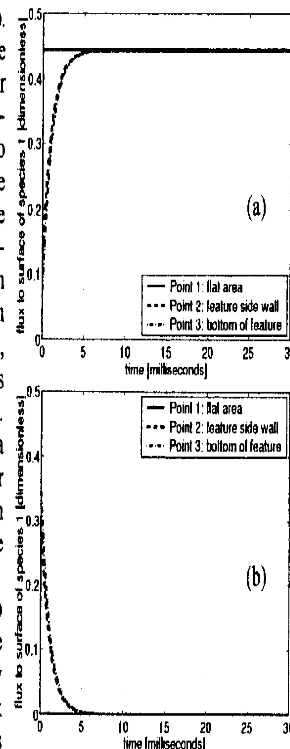

Figure 3. Dimensionless flux of species A to the surface vs. time during (a) adsorption, (b) post-adsorption purge.

During the reaction step, we seek to investigate the effect ions may have on the deposition rate of TaN. Ions are highly directed species, and the source flux distribution for ions is very narrow. This would lead to very large fluxes of ions at middle of the bottom of the feature as compared to the sidewalls. If the deposition rate due to ions depends on the ion flux, then we would see nonconformal deposition inside the feature if the ions contributed significantly to the deposition rate. However, Park *et al.* [15] state that the films grown by PEALD show excellent step coverage, and there is no variation depending on position within features, i.e., the growth is the same at the bottom and sidewalls. This leads us to conclude that the ion fluxes do not directly affect the deposition rates. Park *et al.* indicate that ions affect the film properties (especially film density) by inducing rearrangement of the atomic layers of TaN. Since we are interested in predicting deposition rates in ALD and PEALD, we focus on the reaction between hydrogen radicals and TBTDET as being the sole reaction affecting the fraction of monolayers deposited per PEALD cycle.

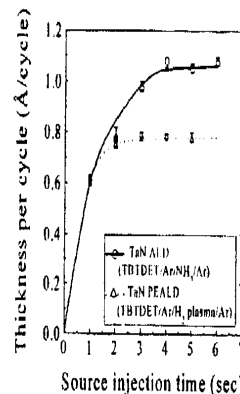

Figure 4. Dependence of deposited film thickness on TBTDET pulse time for TaN ALD using NH_3 and TaN plasma-enhanced ALD using hydrogen plasma (reproduced from [15]).

in closed form, because its coefficients depend on the fluxes η. However, if we can justify the assumption that the fluxes are constant in time, an analytic solution for the fractional coverage θ_k can be obtained (see [10, 11]).

RESULTS

The experimental data we calibrate our model against were obtained from Park *et al.* [15], who conducted a comparison of ALD using NH_3 as the reducing agent, and (hydrogen) plasma enhanced ALD. To ignite and maintain the hydrogen plasma synchronized with the deposition cycle, a rectangular shaped pulse of power was applied between the upper and lower electrode. The lower electrode, on which a wafer resided, was grounded. The upper electrode was of a showerhead type to distribute reactant gases uniformly, and was operated at 50-150 W power, capacitively coupled with an rf (13.56 MHz) power generator [15].

In the experiments reported by Park *et al.* [15], TBTDET was used as the precursor. It was contained in a bubbler that was heated to 70 °C; argon was used as the carrier gas, at a flow rate of 35 cm^3/min. One deposition cycle consisted of an exposure to TBTDET, a purge period with an argon flow rate of 35 cm^3/min, an exposure to hydrogen plasma, followed by another purge period with an argon flow rate of 35 cm^3/min. The hydrogen flow rate was fixed at 75 cm^3/min during the hydrogen plasma pulse. The deposition temperature was 260 °C, and the deposition pressure was 1 Torr. For the case of ALD, ammonia was used as the reducing agent in place of hydrogen radicals. The flow rate of NH_3 was fixed at 47 cm^3/min. The TBTDET pulse time was varied between 1 s and 6 s. All the purge times were 15 s long, and the NH_3 and hydrogen plasma pulses were 10 s long in ALD and PEALD, respectively. The reference concentration and speed of TBTDET at these conditions are 1.5 x 10^{-9} mol/cm^3 and 1.05 x 10^4 cm/s respectively.

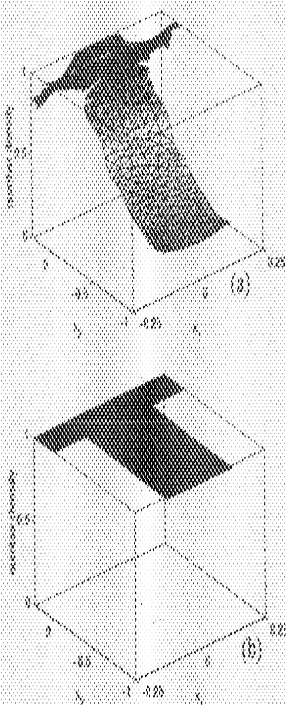

Figure 2. TBTDET adsorption step: dimensionless number density of species A for a feature with aspect ratio A = 4 at (a) 5.0 ns, (b) 40.0 ns. The scales on the x_1 and x_2 axes are different.

Figures 2a and 2b show representative distributions of the dimensionless number density of TBTDET throughout the gas domain during the adsorption step at t = 5 ns and 40 ns. After 5 ns, the gas has not filled the interior of the feature yet; after 40 ns the feature has filled completely with gas. This demonstrates that the transport is much faster than the duration of the adsorption step. Similarly, the gas is transported out of the feature domain over a time scale much shorter than the duration of the pulse during the post-adsorption purge. Figure 3 shows the flux to the surface of species A vs. time at the three observation points (see Fig. 1), Fig. 3a for the adsorption step and Fig. 3b for the post-adsorption purge step. Observe that in both processing steps, the flux tends to equilibrium more slowly than the gas fill of the domain, but significantly faster than the total step times for adsorption and post-adsorption purge. Additionally, observe that the fluxes tend to a spatially uniform constant value. For similar and more detailed results on the adsorption and post-adsorption purge steps of ALD, see Ref. 10.

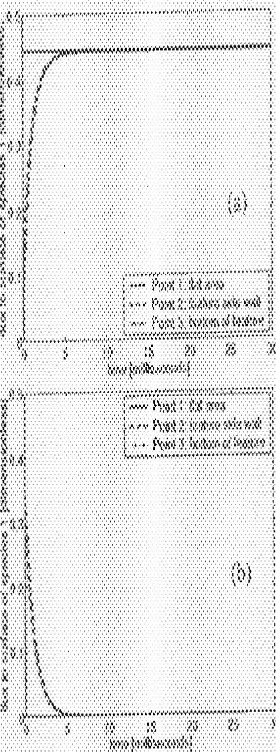

Figure 3. Dimensionless flux of species A to the surface vs. time during (a) adsorption, (b) post-adsorption purge.

During the reaction step, we seek to investigate the effect ions may have on the deposition rate of TaN. Ions are highly directed species, and the source flux distribution for ions is very narrow. This would lead to very large fluxes of ions at middle of the bottom of the feature as compared to the sidewalls. If the deposition rate due to ions depends on the ion flux, then we would see nonconformal deposition inside the feature if the ions contributed significantly to the deposition rate. However, Park *et al.* [15] state that the films grown by PEALD show excellent step coverage, and there is no variation depending on position within features, i.e., the growth is the same at the bottom and sidewalls. This leads us to conclude that the ion fluxes do not directly affect the deposition rates. Park *et al.* indicate that ions affect the film properties (especially film density) by inducing rearrangement of the atomic layers of TaN. Since we are interested in predicting deposition rates in ALD and PEALD, we focus on the reaction between hydrogen radicals and TBTDET as being the sole reaction affecting the fraction of monolayers deposited per PEALD cycle.

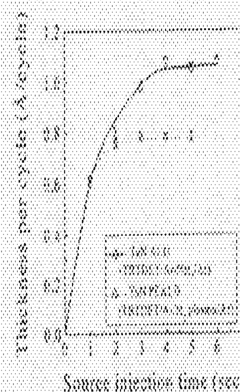

Figure 4. Dependence of deposited film thickness on TBTDET pulse time for TaN ALD using NH_3 and TaN plasma-enhanced ALD using hydrogen plasma (reproduced from [15]).

Similar to the results for TBTDET in the adsorption step, the transport of hydrogen radicals during the reaction step is fast compared to surface kinetics, and the radical flux reaches a spatially uniform constant value in the order of milliseconds. Given this fact, we can use the analytical solution developed in Refs. 10 and 11 to track monolayer coverage and deposition rates over many ALD cycles and as a function of pulse times.

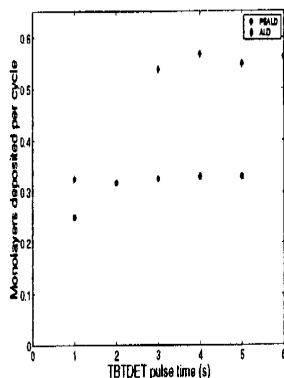

Figure 5. Monolayers deposited per cycle for TaN ALD using NH_3 and TaN PEALD using a hydrogen plasma [15].

Figure 4 shows the experimental data relating deposition thickness per cycle to TBTDET pulse time for TaN ALD and PEALD reported by Park *et al.* [15]. As mentioned earlier in this section, all the purge times were 15 s long, and the NH_3 and hydrogen plasma pulses were 10 s long in ALD and PEALD respectively. The deposition rate in PEALD is lower than that in ALD using NH_3 as a reactant. However, the density of TaN film deposited using PEALD (7.9 g cm^{-3}) is larger than that of TaN deposited using ALD with NH_3 (3.6 g cm^{-3}). Figure 5 shows the deposition thickness in monolayers per cycle for PEALD and ALD for the values of deposition thickness in Angstrom/cycle shown in Fig. 4.

We fit the kinetic parameters in our model for surface coverage of adsorbed species to match the dependence of monolayers deposited per cycle on TBTDET pulse time for PEALD and ALD respectively. Since Park *et al.* [15] postulate that the adsorption rate of TBTDET on a hydrogen radical terminated film is different than its adsorption rate on a NH_3 terminated film, we do not force the adsorption and desorption rate parameters to be the same values in both cases. The values obtained for the kinetic parameters are $\gamma_1^f=6.0 \times 10^{-3}$ for the adsorption rate constant, $\gamma_1^b=1.2 \times 10^{-4}$ for the desorption rate constant, $\gamma_2^f=5.1 \times 10^{-1}$ for the reaction rate constant in PEALD, and $\gamma_1^f=3.4 \times 10^{-3}$ for the adsorption rate constant, $\gamma_1^b=6.0 \times$

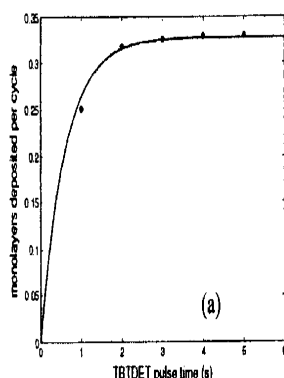

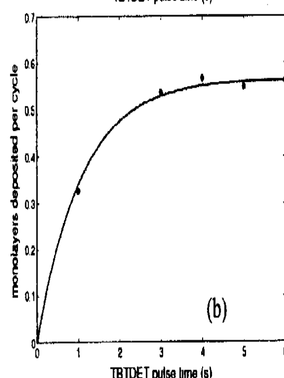

Figure 6. Comparison of model predicted monolayers deposited per cycle against experimental data from [15] for (a) PEALD, (b) ALD.

10^{-5} for the desorption rate constant, $\gamma_2^f=2.9 \times 10^{-1}$ for the reaction rate constant in ALD using NH_3. The model predictions using these fitted parameters are plotted against the experimental data from [15] in Fig. 6. Good agreement is achieved between the fitted model predictions and experimental data. The reaction rate parameter is higher for reaction between adsorbed TBTDET and hydrogen radicals than for reaction between TBTDET and NH_3, indicating that hydrogen radicals are more reactive than NH_3 in this situation. Also, the adsorption rate parameter for TBTDET is higher when hydrogen radicals are present, which is in agreement with the conclusions of Park *et al.* [15]. The higher adsorption rate results in a faster saturation time of monolayers deposited per cycle with respect to TBTDET pulse time. As an explanation of the higher adsorption rate, Park *et al.* [15] suggest that hydrogen radicals would help convert C-H species generated in the hydrogen reduction reaction of TBTDET to be converted to more volatile C-H compounds, which may prevent by-products from residing on the film surface and thus provide more vacant sites for adsorption.

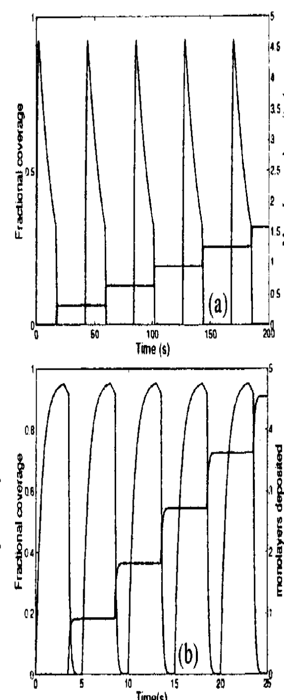

Figure 7. Fractional coverage and monolayers deposited during PEALD for (a) pulse cycle of Park *et al.* [15], and (b) shortened pulse cycle.

Based on our fits of the kinetic parameters of the chemistry models, we predict fractional coverage and monolayers deposited over 5 PEALD cycles. Figure 7*a* shows fractional coverage and monolayers deposited for the pulse cycle used by Park *et al.*; significant loss of coverage due to desorption is observed. The fractional coverage of TBTDET drops from approximately 0.9 to 0.35 during the post-adsorption purge in each ALD cycle. Additionally, the adsorbed TBTDET is consumed by reaction during the first 1 s of the reaction step; there is no deposition during the rest of the reaction step. In the post-reaction purge, the reactants are purged out of the feature domain on the order of milliseconds. This indicates that the purges and the reaction step can be shortened to increase monolayer deposition per unit time. Shortening the post-adsorption purge reduces the loss of adsorbed TBTDET due to desorption, and keeps surface coverage high at the start of the reaction step. Reducing the durations of the reaction step and the post-reaction purge does not affect the monolayer deposition, but results in shortening the duration of the ALD cycle. Figure 7*b* shows predictions of fractional coverage and monolayers deposited when the purge times are shortened to 0.5 s, and the reaction step is shortened to 1 s. The duration of the PEALD cycle is considerably shortened, and approximately 0.9 monolayers are deposited per cycle. The contribution of desorption to

consumption of adsorbed TBTDET is significantly reduced, and almost all the adsorbed TBTDET is consumed by reaction.

In Fig. 8, we show predictions of fractional coverage and monolayers deposited over 5 cycles for TaN ALD using NH_3 as the co-reactant. . Figure 8*a* shows fractional coverage and monolayers deposited for the pulse cycle used by Park *et al.*; significant loss of coverage due to desorption is observed, as was the case with PEALD. Significant desorption during the post-adsorption purge is observed here in Fig. 8*b*, the fractional coverage drops from approximately 0.9 to 0.55. As in the case of TaN PEALD, the reaction and post-reaction purge steps are too long, and can be shortened significantly. Figure 8*b* shows predictions of fractional coverage and monolayers deposited when the purge times are shortened to 0.5 s, and the reaction step is shortened to 1 s. Approximately 0.9 monolayers are deposited per cycle, and one cycle is 6 s long as opposed to 44 s for the original pulse protocol. Notice that for the "optimal" pulse protocols for PEALD and ALD depicted in Figs. 7*b* and 8*b*, approximately the same fraction of a monolayer of TaN is deposited per cycle; the two processes are roughly equivalent in this respect. However, the film densities are different for the two cases, which means that a different thickness of TaN is deposited per cycle in each case. Additionally, Park *et al.* state that properties of the deposited film (such as resistivity) are different for the two processes.

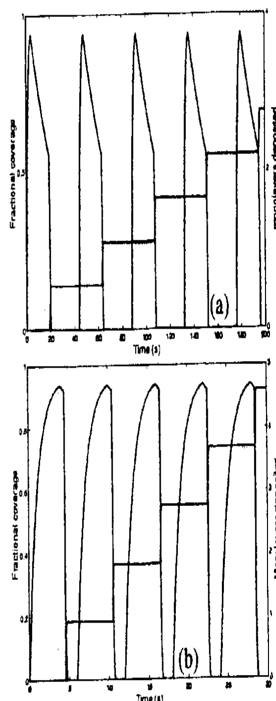

Figure 8. Fractional coverage and monolayers deposited during ALD using NH_3 for (a) pulse cycle of Park *et al.* [15], and (b) shortened pulse cycle.

We have not made any attempt to study the constraints placed on the system by process limitations. We do not know if the durations specified for the reaction step and the purges can be achieved using the processing equipment used by Park *et al.* [15]. In addition to the fast switching between process streams required to keep the purge times as low as 0.5 s, the pulsing of the plasma also needs to be achieved in 1 s. Therefore, our recommendations of the optimal pulse sequences shown in Fig. 7*b* and Fig. 8*b* are subject to the ability of the physical process to be operated in such a fashion. The recommendations are also subject to our surface chemistry model being a good representation of the actual chemistry of the process; a good fit between our model and the data does not necessarily mean that our chemistry model is correct.

CONCLUSIONS

We use a previously developed transient, Boltzmann equation based transport and reaction model to simulate plasma-enhanced ALD and to explain growth rate dependence on pulse times for two different processes for TBTDET sourced TaN recently reported in the literature [15]; ALD using ammonia as the co-reactant and plasma-enhanced ALD using a hydrogen plasma. We use the calibrated chemistry models to predict surface coverage and monolayers deposited over several ALD cycles, and to optimize pulse protocols. We conclude that the monolayers per cycle can be increased relative to the experimental data by shortening the post-adsorption purge time; this decreases reactant desorption. The overall growth rate can by increased by decreasing co-reactant and post-reaction purge pulse times; they are too long. Finally, we conclude that with the improved pulse protocols, the two processes produce approximately the same fraction of monolayer deposited per cycle. This and other details of the coverage and monolayers deposited per cycle depend somewhat on the chemistry model (framework) used. Though the model we use does allow fairly good fits to the available data, this does not mean we have a good chemistry model. The available data are limited and very smooth, and we expect that other models would also provide good fits. The model used seems to be the simplest model that does provide good fits to the data.

ACKNOWLEDGMENTS

The RPI authors acknowledge support from MARCO, DARPA, and NYSTAR for the Interconnect Focus Center.

REFERENCES

[1] M. Ritala and M. Leskela, Nanotechnology, **10**, 19 (1999).
[2] M. Leskela and M. Ritala, J. Phys. IV, Colloq. C5, **5**, 937 (1995).
[3] T. Suntola, Thin Solid Films, **216**, 84 (1992).
[4] H. Siimon and J. Aarik, J. Phys. D: Appl. Phys., **30**, 1725 (1997).
[5] J.-W. Lim, H.-S. Park, and S.-W. Kang, J. Electrochem. Soc., **148** (6), C403 (2000).
[6] H.-S. Park, J.-S. Min, J.-W. Lim, and S.-W. Kang, Applied Surface Science, **158**, 81 (2000).
[7] T. S. Cale, T. P. Merchant, L. J. Borucki, and A. H. Labun, Thin Solid Films, **365**, 152 (2000).
[8] EVOLVE is an extensible topography simulation framework. EVOLVE 5.0i was released in June 1999. © 1991-2001, T. S. Cale.
[9] M. K. Gobbert and T. S. Cale. In: M. T. Swihart, M. D. Allendorf, and M. Meyyappan, editors, *Fundamental Gas-Phase and Surface Chemistry of Vapor-Phase Deposition II*, The Electrochemical Society Proceedings Series, vol. 2001-13, pp. 316-323, 2001.
[10] M. K. Gobbert, S. G. Webster, and T. S. Cale, J. Electrochem. Soc., in press.
[11] M. K. Gobbert, V. Prasad, and T. S. Cale, Thin Solid Films, in press.

[12] M. K. Gobbert, V. Prasad, and T. S. Cale, J. Vac. Sci. Technol. B, in press.
[13] S. M. Rossnagel, A. Sherman, and F. Turner, J. Vac. Sci. Technol. B, **18**(4), 2016 (2000).
[14] J.-S. Park, M.-J. Lee, C.-S. Lee, and S.-W. Kang, Electrochem. Solid-State Lett., 4(4), C17 (2001).
[15] J.-S. Park, H.-S. Park, and S.-W. Kang, J. Electrochem. Soc., **149**(1), C28 (2002).

HIGH-DENSITY PLASMA DEPOSITED SILICON NITRIDE FILMS FOR COATING InGaAlAs HIGH-POWER LASERS

R. E. Sah [1], F. Rinner, R. Kiefer, M. Mikulla, and G. Weimann

Fraunhofer-Institut für Angewandte Festkörperphysik,
Tullastrasse 72, D-79108 Freiburg, Germany
[1] Corresponding author, e-mail address: sah@iaf.fhg.de

Silicon nitride (SiN) films deposited using electron cyclotron resonance plasma-enhanced chemical vapor deposition (ECR-PECVD) technique have been used as optical coatings for the emitting facet of InGaAs/AlGaAs high-power lasers. The films were deposited at 90 °C from a mixture of Ar, N_2 and SiH_4 as precursors. The most important properties of the films are low intrinsic stress and a negligible hysteresis in stress upon thermal cycling. Pre-cleaning of the surface to be coated, and the stable low stress in the film used for coating have been found to be highly valuable for the reliability of InGaAs/AlGaAs high-power lasers.

INTRODUCTION

Passivation and optical coatings are vital for reliable III/V -based diode lasers [1-3]. The most common deposition technique used for these purposes is ion-beam sputtering. With this technique surface damage due to the sputtering atoms may occur [4-6]. The application of the conventional PECVD technique, which uses a parallel-plate type reactor, has also been reported [7-8], but only with limited success until now. Films used for optical coatings, deposited either using the ion-beam technique or the conventional PECVD technique, often contain oxygen. The most important reason for the incorporation of oxygen is to vary the refractive index of the films in a desired range. The incorporated oxygen in the films may affect the long-time stability and reliability [9-11] of the devices. Furthermore, films deposited using conventional PECVD technique at room-to-moderate substrate temperatures (25-250°C) contain hydrogen (H) up to 39 at.% [12,13]. The large amount of H in the films may affect the durability of the coatings specially when a considerable amount is not chemically bonded. The non-bonded H atoms are very likely to desorb when high-power devices are in operation for a long time.

High-density plasma sources such as electron cyclotron resonance (ECR) plasma [14] and inductively coupled plasma (ICP) [15] are increasingly used for the deposition of silicon nitride (SiN) thin films for various purposes in the fabrication of semiconductor electronic and optoelectronic devices. The ECR-PECVD technique provides low ion-